

# Compact Analysis of 3D Bipedal Gait Using Geometric Dynamics of Simplified Models

Stefano Stramigioli  
University of Twente  
Enschede, The Netherlands  
*s.stramigioli@ieee.org*

Vincent Duindam  
EECS, UC Berkeley  
Berkeley, CA, USA  
*v.duindam@ieee.org*

Gijs van Oort  
University of Twente  
Enschede, The Netherlands  
*g.vanoort@utwente.nl*

Ambarish Goswami  
Honda Research Institute  
Mountain View, CA, USA  
*agoswami@honda-ri.com*

**Abstract**—The large number of degrees of freedom in legged robots give rise to complicated dynamics equations. Analyzing these equations or using them for control can therefore be a difficult and non-intuitive task. A simplification of the complex multi-body dynamics can be achieved by instantaneously reducing it to an equivalent single inertial entity called the *locked inertia* or the *composite rigid body inertia*.

In this paper, we adopt the methods of geometric dynamics to analyze the gait using the locked inertia of the robot. The analysis includes the rolling of a biped on a 3D rigid foot and 3D impacts. An example of numerical optimization of foot shape parameters is shown.

Our long-term objective is to develop the theoretical framework and to provide the necessary tools for systematic analysis, design, and control of efficient biped robots.

## I. INTRODUCTION

The fundamental nature of locomotion has been compactly captured as “a question of relating internal shape changes to net changes in position via a coupling mechanism, most often either through interaction with the environment or via some type of conservation law.” [1] The use of geometric tools has been found to be very useful in generating insights into the complex dynamics of locomotion systems. Geometric dynamics is a coordinate-neutral framework which yields results only pertaining to the physics of the system.

The utility of reduced models that capture the essentials of gait dynamics is widely acknowledged. Simple biped models such as the different variations of the inverted pendulum models have been proven immensely beneficial for the study of gait and balance both for humans [2], [3], [4], [5] and humanoid robots [6], [7], [8], [9].

Reduced humanoid models allow one to ignore the non-central aspects of dynamics and to express the complex gait dynamics in a minimalist way. While at the final implementation stage one still needs to formulate control laws for the entire system, it is at the analysis and planning stage where such reduced models demonstrate their value. These models not only enhance our understanding of bipedal locomotion, but open the way to new classes of control laws, which would otherwise be difficult or impossible to conceive.

Many studies have been performed for 2D passive dynamic walkers, starting with the ground-breaking work of McGeer [10], and later on with various systematic approaches, e.g., based on Poincaré mappings [11], [12] and

passivity [13], [14]. Several successful three-dimensional walking robots have been built as well [15], [16], [17], but most of these results were achieved relying more in engineering insight and smart designs rather than systematic analytical methods. The main difficulty when trying to use analytic methods for 3D robots is the sheer complexity of the mechanisms and their interaction with the 3D world.

Our present approach to tackling the complexity of 3D walking robots relies on the very useful concept of *locked inertia* [1], more commonly known in robotics as the *composite rigid body inertia* [18]. The locked inertia of a humanoid robot is its instantaneous generalized inertia, assuming that all of its joints are frozen. It has the same structure as the generalized inertia of a single rigid body. We have recently shown [19] how using this concept an entire humanoid can be mapped into the much simpler entity called the Reaction Mass Pendulum (RMP). In the present paper the instantaneous locked inertia is used to model and to analyze the 3D gaits of humanoid robots including continuous dynamics, foot-ground impacts, and natural rolling motion of curved feet on a support surface.

The paper is structured as follows: Section II presents a general form of the dynamic equations of a walking robot and defines its locked inertia. Section III introduces a geometric description of 3D impacts. Section IV presents the main contribution of this paper. It shows how the previous concepts can be used to analyze and possibly to design the different phases of 3D gait of bipedal robots with curved feet. In Section V we present in a simulation example the optimization of foot shape parameters, using the theory of Section IV.

## II. DYNAMICS OF A HUMANOID

A rigid body is characterized by its *inertia tensor*, which is a second order covariant positive definite tensor. This tensor has a constant numerical representation in any coordinate frame  $\Psi_b$  rigidly connected to the body (often called a body-fixed frame). Furthermore, if the frame is chosen with the origin at the center of mass and with the axes oriented along the principal axes of inertia, the matrix representation of this tensor becomes a  $6 \times 6$  diagonal matrix of the form:

$$\mathcal{I}_i^b = \begin{pmatrix} J & 0 \\ 0 & mI_3 \end{pmatrix} \quad (1)$$

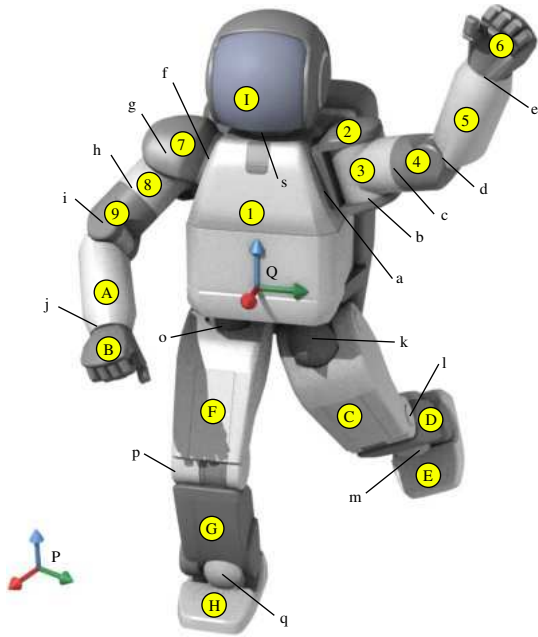


Fig. 1. Setup and labeling of the  $n$  bodies and  $n-1$  joints  $q_i$  in a general free-floating humanoid mechanism. Frame  $\Psi_0$  is the inertial frame,  $\Psi_1$  is attached to the torso, serving as a (non-inertial) reference frame.

where  $\mathcal{I}_i^b$  denotes the inertia tensor of body  $i$  expressed in frame  $\Psi_b$ ,  $m$  is the mass of the body, and the elements of

$$J := \begin{pmatrix} J_x & 0 & 0 \\ 0 & J_y & 0 \\ 0 & 0 & J_z \end{pmatrix}$$

describe the magnitudes of moments of inertia around the three coordinate axes. If only the rotational dynamics are of interest, usually just the  $3 \times 3$  tensor  $J$  is considered.

Consider now a floating mechanism composed of multiple rigid bodies, for example, a humanoid robot floating in space, as shown in Fig. 1. Let us index the bodies  $i \in \{1, \dots, n\}$ , rigidly attach a frame  $\Psi_i$  to each body  $i$ , and align the frame axes with the principal inertia axes.  $\mathcal{I}_i^i$  is the (constant) inertia of body  $i$  expressed in  $\Psi_i$ . In addition, let  $\Psi_0$  denote an inertial (world) frame.

#### A. Locked Inertia

If we lock all joints of this mechanism, we can calculate the total inertia of the entire mechanism in a static configuration just by summing the inertia tensors of the composing rigid bodies (since inertia is additive); this is the locked inertia of the mechanism. Expressing the locked inertia  $\mathcal{I}_{\text{tot}}^j$  in some arbitrary coordinate frame  $\Psi_j$ , we can write

$$\mathcal{I}_{\text{tot}}^j = \sum_{i=1}^n \mathcal{I}_i^j = \sum_{i=1}^n \text{Ad}_{H_i^j}^T \mathcal{I}_i^i \text{Ad}_{H_i^j} \quad (2)$$

where  $\text{Ad}_{H_i^j}$  is the adjoint of the homogeneous transformation  $H_i^j$  from frame  $\Psi_i$  to frame  $\Psi_j$  [20], [21]. Similar to that of a single rigid body, the locked inertia also possesses principal axes, and for a proper choice of coordinate frames, can be expressed in the simple form of Eq. 1. Therefore, once

the joints are physically locked, the floating mechanism will obey the dynamics of a single rigid body with inertia  $\mathcal{I}_{\text{tot}}^j$ .

#### B. Dynamic Equations of a General Mechanism

Suppose that we have a general humanoid mechanism composed of an interconnection of rigid bodies. If we take one of the rigid bodies (typically a foot or the torso) as a reference with frame  $\Psi_1$  (the base frame), the internal configuration or “shape” of the humanoid is completely defined by a set of joint coordinates  $q$ . The total configuration of the robot is thus given by the configuration  $H_1^0 \in \text{SE}(3)$  of the reference frame plus the internal joint angles  $q \in \mathbb{R}^n$ . Similarly, a certain kinematic state of the system can be characterized by the twist  ${}^1T_1^0 \in \text{se}(3)$  of the reference body plus the joint velocities  $\dot{q} \in \mathbb{R}^n$ , where  ${}^cT_a^b \in \text{se}(3) \sim \mathbb{R}^6$  denotes the twist of body  $a$  with respect to body  $b$  expressed in coordinate frame  $\Psi_c$ . The reference body twist and the joint velocities can be combined in a vector of the form

$$\bar{T} := \begin{pmatrix} {}^1T_1^0 \\ \dot{q} \end{pmatrix} \quad (3)$$

For each body  $i$  we can write its twist as

$${}^iT_i^0 = {}^iT_1^0 + {}^iT_i^1 = \text{Ad}_{H_1^i(q)} ({}^1T_1^0 + J_i(q)\dot{q}) \quad (4)$$

with  $J_i(q)$  the geometric Jacobian mapping the internal shape speed to the twist of body  $i$  with respect to the reference body 1 expressed in frame  $\Psi_1$ . In particular,  $J_1(q) \equiv 0$  by construction.

Using these coordinates, we can write an expression for the kinetic co-energy as

$$E^*({}^1T_1^0, q, \dot{q}) = \frac{1}{2} \bar{T}^T M(q) \bar{T} \quad (5)$$

where the mass matrix  $M(q)$ , which is independent of  $H_1^0$ , has the following structure:

$$M(q) := \begin{pmatrix} \sum \text{Ad}_{H_1^i}^T \mathcal{I}_i^i \text{Ad}_{H_1^i} & \sum \text{Ad}_{H_1^i}^T \mathcal{I}_i^i \text{Ad}_{H_1^i} J_i \\ \sum J_i^T \text{Ad}_{H_1^i}^T \mathcal{I}_i^i \text{Ad}_{H_1^i} & \sum J_i^T \text{Ad}_{H_1^i}^T \mathcal{I}_i^i \text{Ad}_{H_1^i} J_i \end{pmatrix} \quad (6)$$

The top-left  $6 \times 6$  sub-matrix is seen to be exactly the locked inertia of Eq. 2 expressed in  $\Psi_1$ . Using the Boltzmann-Hamel equations we can then obtain the dynamics equations of the mechanism (see [22] for the details):

$$\dot{P}^1 = \text{ad}_{({}^1T_1^0)}^T P^1 + \sum_{i=1}^n {}^iW_i \quad (7)$$

$$\dot{p} = \gamma(q, \dot{q}, {}^1T_1^0) + \tau + \sum_{i=1}^n J_i^T {}^iW_i \quad (8)$$

where  ${}^jW_i$  indicates the total external wrench applied to body  $i$  expressed in frame  $\Psi_j$ ,  $\tau_i$  indicates the torque applied at joint  $i$ ,  $P^i$  indicates the total momentum screw expressed in frame  $i$ , and  $\gamma$  is a vector of all Coriolis, centrifugal, and other nonlinear internal forces.  $p$  is the  $n \times 1$  vector of generalized momentum coordinates such that

$$\bar{P} := \begin{pmatrix} P^1 \\ p \end{pmatrix} = M \bar{T} \quad (9)$$

For a free-floating humanoid with locked joints, the dynamics of Eq. 7 are equivalent to the dynamics of a single rigid body with inertia equal to the locked inertia, and Eq. 8 becomes void. The structure of the presented equations clearly separates the internal (Eq. 8) from the external dynamics (Eq. 7).

### III. IMPACTS

When a foot of the robot touches the ground, an impact occurs. This is characterized by certain velocities, *i.e.*, the linear velocities of the impact point, instantaneously reducing to zero. In this section we first derive a projection matrix relating the pre-impact momentum to the post-impact momentum. Then, we show that also during impact, a locked multi-body chain behaves as a single rigid body.

#### A. Single Impacts on a Rigid Mechanism

Since the complete kinematic state of the robot is described using  $\bar{T}$ , the velocity  $\dot{s}$  of any point on any of the bodies in the mechanism can be expressed as:

$$\dot{s} = A(q)\bar{T} \quad (10)$$

where we can assume  $A(q)$  a full row rank matrix. By construction, we will have for the velocity just after impact  $\dot{s}_+ = 0$ , although in general the velocity just before impact  $\dot{s}_- \neq 0$ . The dual impulsive force on the mechanism will be of the form:

$$\begin{pmatrix} W \\ \tau \end{pmatrix} = A^T(q)\lambda\delta(t) \quad (11)$$

where  $\lambda$  is the magnitude of the impulsive force and  $\delta(t)$  indicates a Dirac pulse at  $t = 0$ , which, without loss of generality, we assume to be the time of impact. The impulsive force of Eq. 11 applied to the dynamics of Eq. 7 and Eq. 8 can be written as:

$$\bar{P}_+ - \bar{P}_- = A^T(q)\lambda. \quad (12)$$

Where subscript  $-$  denotes the time just before impact, and subscript  $+$  the time just after impact.

Pre-multiplying by  $M^{-1}$  as defined in Eq. 6 we get

$$\bar{T}_+ - \bar{T}_- = M^{-1}A^T\lambda \quad (13)$$

which, pre-multiplied by  $A$  and using  $\dot{s}_+ = 0$ , gives

$$-A\bar{T}_- = AM^{-1}A^T\lambda \quad (14)$$

and finally, since  $M$  is positive definite and  $A$  has full row rank, we obtain an expression for  $\lambda$  as

$$\lambda = -(AM^{-1}A^T)^{-1}AM^{-1}\bar{P}_- \quad (15)$$

which can be substituted into Eq. 12 to obtain the total momentum projection operation:

$$\bar{P}_+ = \mathbb{P}(q)\bar{P}_- \quad (16)$$

with projection matrix  $\mathbb{P}(q)$  equal to

$$\mathbb{P}(q) := I - A^T(AM^{-1}A^T)^{-1}AM^{-1}. \quad (17)$$

This is a projection matrix acting on the momentum vector, but we can directly define the following projection  $\mathbb{P}_T(q)$  acting on the velocity vector  $\bar{T} = M^{-1}\bar{P}$ .

$$\mathbb{P}_T(q) := I - M^{-1}A^T(AM^{-1}A^T)^{-1}A \quad (18)$$

such that  $\bar{T}_+ = \mathbb{P}_T(q)\bar{T}_-$ .

#### B. Impacts in a Locked Mechanism

When the mechanism is locked and there is an external impact, intuitively it should behave like the single equivalent rigid body with inertia equal to the locked inertia. To prove this, we can write the impact constraints and equations of Eq. 10 as a set of two impact constraints: one is the impact from the ground forces, and one is the impulsive joint torques required to keep the joint velocities to zero:

$$\begin{pmatrix} \dot{s} \\ \dot{q} \end{pmatrix} = \begin{pmatrix} A_1(q) \\ A_2(q) \end{pmatrix} \bar{T} = \begin{pmatrix} A_{11}(q) & A_{12}(q) \\ 0 & I \end{pmatrix} \begin{pmatrix} {}^1T_1^0 \\ \dot{q} \end{pmatrix} \quad (19)$$

Following the same derivations as before, we obtain an equation like Eq. 13:

$$\bar{T}_+ - \bar{T}_- = M^{-1} \begin{pmatrix} A_{11}^T & 0 \\ A_{12}^T & I \end{pmatrix} \begin{pmatrix} \lambda_c \\ \lambda_i \end{pmatrix} \quad (20)$$

with subscript  $c$  for contact and  $i$  for internal. We first express the required internal locking torques  $\lambda_i$  as a function of  $\lambda_c$ , and then compute the external impact forces  $\lambda_c$ . Starting with the second constraint (internal locking), we pre-multiply Eq. 20 by  $A_2$  and using the assumption that  $\dot{q}_- = 0$  (the mechanism is locked before ground impact) to write

$$0 = -\dot{q}_- = \begin{pmatrix} 0 & I \end{pmatrix} M^{-1} \begin{pmatrix} A_{11}^T & 0 \\ A_{12}^T & I \end{pmatrix} \begin{pmatrix} \lambda_c \\ \lambda_i \end{pmatrix} \quad (21)$$

If we structure the mass matrix of Eq. 6 as

$$M = \begin{pmatrix} F & G \\ G^T & H \end{pmatrix} \quad (22)$$

with  $F$  the locked inertia, and use the linear systems theory of block matrix inverses and Schur Complements [23], we can write the inverse of the mass matrix as

$$M^{-1} = \begin{pmatrix} F^{-1} + F^{-1}GS_F^{-1}G^TF^{-1} & -F^{-1}GS_F^{-1} \\ -S_F^{-1}G^TF^{-1} & S_F^{-1} \end{pmatrix} \quad (23)$$

with  $S_F$  the Schur complement of  $F$ . Substituting this into the right-hand side of Eq. 21, we obtain the relation between  $\lambda_c$  and  $\lambda_i$  as

$$0 = (-S_F^{-1}G^TF^{-1}A_{11}^T + S_F^{-1}A_{12}^T)\lambda_c + S_F^{-1}\lambda_i \quad (24)$$

Continuing now with the first constraint, and again using the assumption that  $\dot{q}_- = 0$ , we pre-multiply Eq. 20 by  $\begin{pmatrix} A_{11} & 0 \end{pmatrix}$  to find

$$-A_{11}({}^1T_1^0)_- = \begin{pmatrix} A_{11} & 0 \end{pmatrix} M^{-1} \begin{pmatrix} A_{11}^T & 0 \\ A_{12}^T & I \end{pmatrix} \begin{pmatrix} \lambda_c \\ \lambda_i \end{pmatrix}. \quad (25)$$

Substituting  $M^{-1}$  from Eq. 23 and expressing  $\lambda_i$  as a function of  $\lambda_c$  using Eq. 21, we obtain

$$-A_{11}({}^1T_1^0)_- = A_{11}F^{-1}A_{11}\lambda_c \quad (26)$$

which shows that, indeed, if the shape velocity  $\dot{q}_-$  before impact equals zero and the mechanism is locked (through the impulsive joint torque  $\lambda_i$ ), then the effect of a ground impact with magnitude  $\lambda_c$  is just Eq. 15 with  $A \rightarrow A_{11}$  and  $M \rightarrow F = \mathcal{I}_{\text{tot}}^1$  (the locked inertia). The momentum projection matrix Eq. 17 follows directly as

$$\mathbb{P}(q) = I - A_{11}^T (A_{11} (\mathcal{I}_{\text{tot}}^1)^{-1} A_{11}^T)^{-1} A_{11} (\mathcal{I}_{\text{tot}}^1)^{-1} \quad (27)$$

#### IV. ANALYSIS OF 3D WALKING CYCLES

We now have all the necessary ingredients to analyze and describe the kinematics and dynamics of 3D walking gaits of (simplified) bipedal robots with curved feet. This section presents equations and relations that apply to the various phases of locomotion. These relations can be used for straightforward simulation of a particular robot, but the ultimate goal is to apply them for optimal *design* of bipeds with specific desired gait properties.

In what follows we make the following assumptions

- 1) The double stance phase is instantaneous,
- 2) All internal joints are locked during impact,
- 3) The feet are perfectly rigid with convex, curved shape,
- 4) The stance foot rolls over the ground without slipping,
- 5) The inertial effect of the swing leg is either negligible or is compensated by proper motion of the torso or arms.

We are aware of the fact that some of these assumptions will not hold in general. Finding ways in which these assumptions (especially 1 and 5) can be relaxed without falling back to the original, complex full dynamics equations is future work.

In the next sub-section we discuss high-level kinematic properties of 3D gaits. After that, kinematics and dynamics of the rolling stance phase are discussed.

##### A. High-level Kinematic Description of 3D Gait

The first aspects of a 3D walking cycle are the high-level kinematic properties. Concepts like walking direction, step length, and foot rolling direction are trivial in 2D walking and reasonably intuitive in 3D, but it is useful to describe the relation of these quantities to kinematic states of the robot, rather than implicitly through definition of a coordinate system with axes aligned in a specific way.

The momentum  $P_+^1$  of a locked biped just after impact can be calculated using Eq. 27 and corresponds to a twist

$$({}^1T_1^0)_+ = (\mathcal{I}_{\text{tot}}^1)^{-1} P_+^1. \quad (28)$$

Under hypotheses 2–4, the motion of the locked biped right after impact will be a rolling motion on the stance foot, following a trajectory that depends on the shape of the foot and  $({}^1T_1^0)_+$ . The rolling motions corresponding to several steps in a symmetric gait are illustrated in Fig. 2. The  $k$ -th impact in the figure corresponds to an impact of the right foot, and the figure shows the moving axis  $\omega_k$  around which the rolling motion occurs. For a slip-less pure rolling contact, the axis  $\omega_k$  must be in the walking plane, orthogonal to the trajectory of the contact point of the foot with the ground.

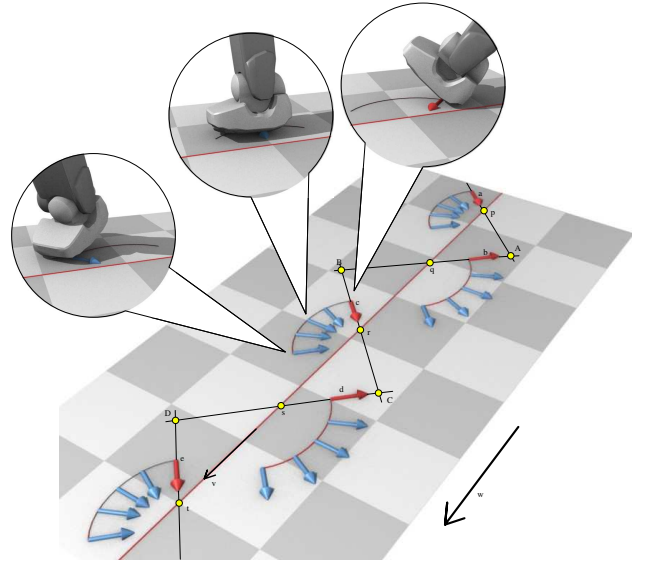


Fig. 2. Geometric description of a symmetric walking gait. The stance foot rolls along a moving axis  $\omega$ , with stride length described by the points  $\bar{p}$ , and  $\hat{v}$  the direction of forward walking.

For a (desirable) symmetric gait, there exists a relation between consecutive steps in the walking cycle (and hence between consecutive rolling axes  $\omega$ ) and the global walking direction. If we denote by  $\mathbf{e}_z$  a unit vector in  $z$ -direction (pointing upwards) and by  $\hat{v}$  the unit vector in the walking direction, it can be seen that

$$\hat{v} = \frac{(\omega_k \times \mathbf{e}_z) + (\omega_{k+1} \times \mathbf{e}_z)}{\|(\omega_k \times \mathbf{e}_z) + (\omega_{k+1} \times \mathbf{e}_z)\|} \quad (29)$$

where  $\times$  denotes the vector product (think of  $\mathbf{e}_z$  as a vector pointing from the ground up to some point of the robot, *e.g.*, the hip, and note that  $\omega \times \mathbf{e}_z$  denotes the linear velocity of that point).

Let us assume that the shape of the curves traced by the contact points is outward, that is, during rolling, the contact points move away from the center line and then return (as in Fig. 2). For efficiency reasons, it is clear that this is a necessary property: through the outward bending shape, the final rolling axis of one foot just before impact will be more or less aligned with the initial rolling axis of the other foot just after impact. In this way, the motion continues reasonably smoothly across impacts and little energy is lost. If the trajectory of the contact point were to bend inward during rolling, the rolling axes just before and after impact would be misaligned, leading to significant energy loss. Because we can design the contact point trajectory ourselves (see Section V), we can design it in such a way that the assumption holds. In that case, we can use a simpler equation for the walking direction, being

$$\hat{v} = \frac{\omega_k + (-\omega_{k+1})}{\|\omega_k + (-\omega_{k+1})\|}. \quad (30)$$

If the locations of the impacts are known, we can define the points  $p_k$  in the figure as the intersections of the lines

defined by the twist axes of two consecutive steps  $k$  and  $k + 1$ . For a symmetric gait, the sequence of middle points

$$\bar{p}_k := (p_k + p_{(k-1)})/2 \quad (31)$$

will lie on a center line in the walking direction  $\hat{v}$ . The distance between subsequent points  $\bar{p}_k$  corresponds to the longitudinal step length. The lateral distance of a point  $p_k$  describes how much the foot trajectories curve away from  $\hat{v}$ , *i.e.*, it depends on  $\langle \hat{v}, \omega_k \rangle$ .

### B. Kinematics of 3D Rolling

Continuing now with the details of the rolling motion during the stance phase, suppose we have decided on a desired walking direction  $\hat{v}$  and rolling twist  $\omega_k$  after impact, and suppose we have chosen a desired trajectory of the contact point on the floor, for example a spline interpolating between the impact point and rolling direction and the release point and rolling direction.

Under these assumptions, we can write down a relation for the kinematics of 3D rolling of the foot such that the contact point between the foot and the floor follows the desired trajectory. If we take  $r$  to be the moving contact point, we know from previous work [24], [25] that

$$(g_{1*} + H_0^1 g_{0*} H_1^0) \dot{r}_1 = {}^1\tilde{T}_0^1 g_1 - H_0^1 g_{0*} {}^0\tilde{T}_1^0 r_0 \quad (32)$$

with  $r_1$  the contact point in body coordinates,  $r_0$  the contact point in floor coordinates,  $g_1$  the normal to the foot surface, and  $g_0$  the normal to the floor. The tangent mappings  $g_{1*}$  and  $g_{0*}$  describe the local curvature of the foot and floor surfaces at the contact point. Since the floor is assumed fully flat  $g_{0*} \equiv 0$  and the previous equation reduces to

$$\dot{g}_1 = g_{1*} \dot{r}_1 = {}^1\tilde{T}_0^1 g_1 = -{}^1\tilde{T}_1^0 g_1 \quad (33)$$

This equation gives a relation between the twist  ${}^1T_1^0$  of the foot and the change  $\dot{g}_1$  of the normal vector to the foot surface, which is equal to the foot curvature  $g_{1*} \dot{r}_1$  in the direction of the trajectory of the contact point. Since  $\dot{r}_1$  must be along the surface of the foot, we have an additional constraint

$$g_1^T \dot{r}_1 = 0 \quad (34)$$

Depending on the purpose of our analysis of the walking cycle, we can read these equations in several ways. First, they give us the possible relative motions  ${}^1T_1^0$  for a given foot surface shape  $g_{1*}$ . It can be seen that these correspond to the three rolling directions around the contact point. Second, for given foot shape  $g_{1*}$  and relative motion  ${}^1T_1^0$ , the equations give us the motion of the contact point  $\dot{r}_1$ . Finally, and this is the most interesting application, Eq. 33 can give us design constraints for the foot: for given desired motions  $\dot{r}_1$  of the contact point and rolling motion  ${}^1T_1^0$ , we can find local surface shapes  $g_{1*}$  that satisfy the equation. Since Eq. 33 only gives us a relation for the curvature in the direction of motion, the curvature in the orthogonal direction can be designed separately, *e.g.*, to increase stability or efficiency of the rolling motion.

### C. Dynamics of 3D Rolling

The next step in the analysis of the stance phase is the dynamics of the rolling motion. Here, we use hypothesis 5 and neglect the inertial effect of the swing leg, or equivalently, we assume its effect is compensated by a counter-effect through motion of the torso or arms. These assumptions allow us to again study the biped through its locked inertia.

Under hypothesis 5, the inertia of the system is constant, hence we study the dynamics of the locked inertia, rolling on the stance foot. In other words, we look at the dynamics of a rigid body with inertia equal to the locked inertia, with surface defined by the foot surface of the stance foot, rolling on a flat floor. As discussed before, the rolling constraint allows only motion around three rotation axes passing through the contact point, and hence we can write the allowed relative twist  ${}^1T_1^0$  of the body with respect to the floor as

$${}^1T_1^0 = X(r)\omega := \begin{pmatrix} T_x(r) & T_y(r) & T_z(r) \end{pmatrix} \begin{pmatrix} w_x \\ w_y \\ w_z \end{pmatrix} \quad (35)$$

with  $T_i(r)$  the twist describing rotation around axis  $i$  located at the contact point  $r$  and  $w_i$  the angular velocity around  $T_i$ . The columns of the matrix  $X(r)$  give a basis for the space of allowed twists. Note that this is similar but opposite to the matrix  $A$  in Eq. 10 which gives a basis for the space of *constrained* velocities.

*Theorem 1:* The dynamics of a locked biped with locked inertia tensor  $\mathcal{I}$ , external wrench  $W$ , and rolling on a foot with allowed twists given by  ${}^1T_1^0$  as in Eq. 35 and moving contact point  $r$ , are given as

$$\bar{\mathcal{I}}\dot{w} + Cw = X^T W \quad (36)$$

with  $\bar{\mathcal{I}} := (X^T \mathcal{I} X)$  and  $C := X^T \mathcal{I} \dot{X} - X^T \text{ad}_{Xw}(\mathcal{I} X)$ .

*Proof:* Since all the joints are locked, the behavior of the biped is the same as the behavior of a single rigid body, and its dynamics are therefore given by the dynamics equation for a rigid body [21]

$$\mathcal{I} \frac{d}{dt} ({}^1T_1^0) - \text{ad}_{{}^1T_1^0}(\mathcal{I} {}^1T_1^0) = W + W_c \quad (37)$$

where  ${}^1T_1^0$  is the twist of the body,  $\text{ad}_{{}^1T_1^0}$  is its algebra representation adjoint, and  $W_c$  are the external wrenches due to the rolling contact with the floor.

Since we can write  ${}^1T_1^0 = X(r)w$  at all times, we can substitute this into Eq. 37 and write

$$\mathcal{I} \frac{d}{dt} (X(r)w) - \text{ad}_{X(r)w}(\mathcal{I} X(r)w) = W + W_c \quad (38)$$

As the contact wrenches  $W_c$  are dual to the allowed twists  $Xw$ , we have by definition  $X^T W_c \equiv 0$ , and hence if we multiply the equation from the left by  $X^T$ , we obtain

$$X^T \mathcal{I} \frac{d}{dt} (Xw) - X^T \text{ad}_{Xw}(\mathcal{I} Xw) = X^T W \quad (39)$$

$$X^T \mathcal{I} X \dot{w} + X^T \mathcal{I} \dot{X} w - X^T \text{ad}_{Xw}(\mathcal{I} Xw) = X^T W \quad (40)$$

$$(X^T \mathcal{I} X) \dot{w} + X^T (\mathcal{I} \dot{X} - \text{ad}_{Xw} \mathcal{I} X) w = X^T W \quad (41)$$

which is the result in the theorem if we substitute the definitions of  $\bar{T}$  and  $C$ . ■

On a practical note, we can express  $\dot{X}$  in terms of the kinematic states  $H_1^0$  and  $w$  as

$$\dot{X} = \frac{\partial X}{\partial r} \dot{r}_1 \quad (42)$$

with  $\dot{r}_1$  the velocity of the contact point. Using Eq. 33, Eq. 34, and the assumption that contact between the floor and the foot occurs only at a single point (since the foot is assumed convex), there is a unique solution  $\dot{r}_1$  that satisfies the following equations

$$g_{1*} \dot{r}_b = -{}^1\tilde{T}_1^0 g_1 = -\widetilde{(Xw)} g_1 \quad (43)$$

$$g_1^T \dot{r}_1 = 0 \quad (44)$$

The theorem gives an explicit differential equation that describes the dynamics of the locked biped (or any rigid body) with arbitrary foot shape and point contact with the ground, as a function of the relative configuration  $H_1^0$  (which determines  $r$ ) and the velocity state  $w$ . The external wrench  $W$  may include forces such as gravity or ankle actuation. Just as the equation for the kinematics of 3D rolling, this equation can be used for different purposes. The most straight-forward way is to use it as a model to predict the motion of a locked biped with a particular foot shape. A more interesting application, however, is to use it to *design* a foot shape, given a certain desired walking gait. As stated in the introduction, it is these applications that benefit most from reduced models such as the one presented here. The dynamics equations are relatively simple, and for a given trajectory (given  $H_1^0$  and  ${}^1T_1^0$  as functions of time), it can be used in optimization routines that adapt the foot shape parameter  $g_{1*}$ . An example is shown in Section V.

For bipedal walking on a horizontal floor, the impacts of the feet with the ground will generally reduce the kinetic energy of the system (except for very specific motions for which the projection operator of Eq. 17 becomes the identity). In order to compensate for this and obtain a cyclic motion, energy needs to be injected into the system. One way that humans inject energy is through the use of ankle push-off. We can mimic this behavior and use an actuator in the ankle to slightly raise the center of mass of the biped at the beginning of each step, thus increasing the potential energy and making a cyclic motion possible. Since the inertia of the foot is small compared to the inertia of the rest of the biped, we can include ankle actuation into the dynamics as part of the external wrench  $W$ .

## V. SIMULATION EXAMPLE

In this section we give a simple example of how the theory of Section IV can be applied for the design of a foot shape. We consider the design as a numerical optimization problem with two parameters.

Consider a system of one rigid body (or, equivalently, a locked system of multiple bodies), having an ellipsoidal foot, as shown in Fig. 3. This system represents the robot's right foot, right leg and torso rigidly attached to each other.

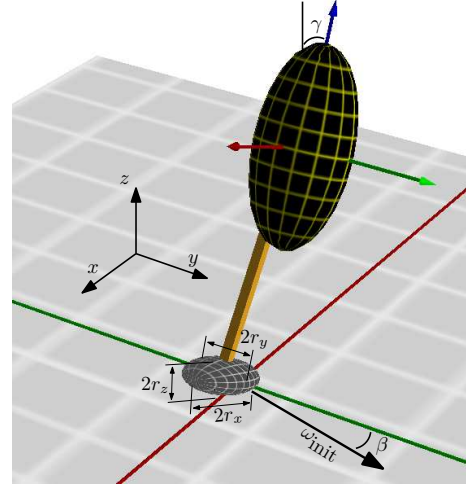


Fig. 3. Simulation model for parameter optimization.

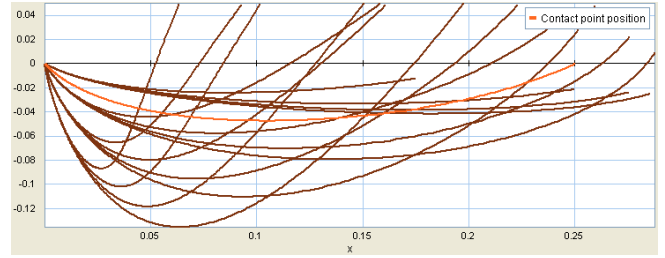


Fig. 4. Foot contact point trails for different parameter values of  $(2r_y) \in [0.1, 0.3 \text{ m}]$  and  $|\omega_{\text{init}}| \in [1.1, 1.6 \text{ rad/s}]$  (dark lines) and the optimal solution as stated in the text (light line).

Our target is to find a foot width  $(2r_y)$  and initial angular velocity magnitude  $|\omega_{\text{init}}|$  that make the foot roll as shown in Fig. 2. We consider only one step and want a step time of  $t_{\text{step}} = 1 \text{ s}$ . As the optimization criterion we use the Euclidean distance  $d$  between the foot's contact point  $r_0(t)$  at  $t = 1 \text{ s}$  and a certain chosen desired contact point location  $r_{0,\text{des}} = [0.25 \ 0 \ 0]^T$  (without loss of generality we chose  $r_0(0) = [0 \ 0 \ 0]^T$ ). The direction of the initial angular velocity  $\beta$ , the length  $(2r_x = 0.3 \text{ m})$  and height  $(2r_z = 0.05 \text{ m})$  of the foot, as well as the inertial properties  $\mathcal{I}$  and initial orientation  $\gamma$  of the body are kept fixed during the experiment. In order to obtain a unique solution, we do not allow rotation around  $w_z$  (see Eq. 35).

We used the simulation package 20-sim [26] to perform an automatic parameter optimization by first making a parameter sweep in both parameters (Fig. 4) and then optimize the best result by a steepest-descent method. The optimal solution was found at  $2r_y = 0.274 \text{ m}$ ,  $|\omega_{\text{init}}| = 1.22 \text{ rad/s}$ . The final contact point  $r_0$  was exactly our desired point  $r_{0,\text{des}}$  ( $d = 0$ ).

Although this is a very simple example, it does show the application of the method. By choosing other optimization parameters and criteria (e.g., incorporating the final orientation of the body or the final direction of  $\omega$ ), we may be able to design feet that maximize aspects like disturbance

rejection during a step, or good performance over a range of gaits.

## VI. CONCLUSIONS AND FUTURE WORK

In this paper we presented a systematic dynamic analysis of 3D bipedal gait. The gait comprises a foot rolling phase and an instantaneous phase of foot/ground impact. We showed how these phases can be analyzed separately and described in approximation using simplified models described by the locked inertia and a momentum projection. The resulting equations are much simpler than the full robot dynamics and can be used as a starting point for analysis and foot shape design.

One feature of this analysis is the use of locked inertia or composite rigid body inertia, which is an instantaneous single rigid body equivalent of the full biped. Using this simplified model makes the complex multi-joint robot dynamics more manageable for theoretical probing. The authors believe that insight from geometric dynamics can potentially lead to a more efficient bipedal gait that exploits natural dynamics.

Our long-term objective is to continue to develop a theoretical framework of biped gait based on geometric dynamics. As applications of this framework, we will address several specific topics. We would like to start from a desired nominal locomotion pattern and compute the required shape of the rigid 3D feet. Furthermore, practical applications require disturbance robustness of gait cycles for which both the foot shape and a proper foot placement strategy need to be devised. Finally, previous research has used concepts such as the energy ellipsoid and momentum sphere to describe the dynamics of a rigid body, and it would be interesting to see how these ellipsoids and spheres change under the influence of rolling motion on a convex foot surface.

## ACKNOWLEDGMENTS

Vincent Duindam is sponsored by the Netherlands Organization for Scientific Research (NWO).

## REFERENCES

- [1] J. E. Marsden and J. Ostrowski, "Symmetries in motion: Geometric foundations of motion control," *Nonlinear Science Today*, 1998.
- [2] V. Inman, H. Ralston, and F. Todd, *Human Walking*. Baltimore: William and Wilkins, 1981.
- [3] R. M. Alexander, "The gaits of bipedal and quadrupedal animals," *International Journal of Robotics Research*, vol. 3, no. 2, pp. 49–59, 1984.
- [4] —, "Three uses for springs in legged locomotion," *International Journal of Robotics Research*, vol. 9, no. 2, pp. 53–61, 1990.
- [5] J. McMahon, "Mechanics of locomotion," *International Journal of Robotics Research*, vol. 3, no. 2, pp. 4–28, 1984.
- [6] S. Kajita and K. Tani, "Study of dynamic biped locomotion on rugged terrain," in *IEEE International Conference on Robotics and Automation (ICRA)*, 1991, Sacramento, CA, pp. 1405–1411.
- [7] S. Kajita, F. Kanehiro, K. Kaneko, K. Fujiwara, K. Yokoi, and H. Hirukawa, "A realtime pattern generator for biped walking," in *IEEE International Conference on Robotics and Automation (ICRA)*, 2002, Washington, DC, pp. 31–37.
- [8] T. Sugihara and Y. Nakamura, "Variable impedant inverted pendulum model control for a seamless contact phase transition on humanoid robot," in *IEEE International Conference on Humanoid Robots (Humanoids2003)*, Oct 2003, Germany.
- [9] T. Komura, A. Nagano, H. Leung, and Y. Shinagawa, "Simulating pathological gait using the enhanced linear inverted pendulum model," *IEEE Transactions on Biomedical Engineering*, vol. 52, no. 9, pp. 1502–1513, 2005, September.
- [10] T. McGeer, "Passive dynamic walking," *International Journal of Robotics Research*, vol. 9, no. 2, pp. 62–82, 1990.
- [11] A. Goswami, B. Thuilot, and B. Espiau, "A study of the passive gait of a compass-like biped robot: symmetry and chaos," *International Journal of Robotics Research*, vol. 17, p. 12, 1998.
- [12] M. Garcia, A. Chatterjee, A. Ruina, and M. Coleman, "The simplest walking model: Stability, complexity and scaling," *ASME Journal of Biomechanical Engineering*, vol. 120, no. 2, pp. 281–288, 1998.
- [13] M. W. Spong and F. Bullo, "Controlled symmetries and passive walking," *IEEE Transactions on Automatic Control*, vol. 50, no. 7, pp. 1025–1031, July 2005.
- [14] V. Duindam and S. Stramigioli, "Port-based control of a compass-gait bipedal robot," in *Proceedings of the 16th IFAC World Congress*, July 2005, electronic proceedings.
- [15] M. Wisse and A. L. Schwab, "A 3d passive dynamic biped with roll and yaw compensation," *Robotica*, vol. 19, pp. 275–284, 2001.
- [16] M. Wisse, "Essentials of dynamic walking — analysis and design of two-legged robots," September 2004.
- [17] S. H. Collins, M. Wisse, and A. Ruina, "A three-dimensional passive-dynamic walking robot with two legs and knees," *International Journal of Robotics Research*, vol. 20, no. 7, pp. 607–615, July 2001.
- [18] M. W. Walker and D. Orin, "Efficient dynamic computer simulation of robotic mechanisms," *ASME Journal of Dynamic Systems, Measurement, and Control*, vol. 104, pp. 205–211, Sept. 1982.
- [19] S.-H. Lee and A. Goswami, "Reaction mass pendulum (RMP): An explicit model for centroidal angular momentum of humanoid robots," in *Proceedings of the International Conference on Robotics and Automation (ICRA)*, April 2007, pp. 4667–4672.
- [20] R. M. Murray, Z. Li, and S. S. Sastry, *A Mathematical Introduction to Robotic Manipulation*. Boca Raton: CRC Press, 1994.
- [21] S. Stramigioli, *Modeling and IPC Control of Interactive Mechanical Systems – A Coordinate-free Approach*. Springer-Verlag, 2001.
- [22] V. Duindam and S. Stramigioli, "Singularity-free dynamic equations of open-chain mechanisms with general holonomic and nonholonomic joints," *IEEE Transactions on Robotics*, vol. 24, no. 3, pp. 517–526, June 2008.
- [23] G. Strang, *Linear Algebra and its Applications*, 3rd ed. Brooks Cole, 1988.
- [24] D. J. Montana, "The kinematics of compliant contact and grasp," *International Journal of Robotics Research*, vol. 7, no. 3, pp. 17–32, 1989.
- [25] V. Duindam and S. Stramigioli, "Modeling the kinematics and dynamics of compliant contact," in *Proceedings of the International Conference on Robotics and Automation*, September 2003, pp. 4029–4034.
- [26] "20-sim version 4.0," <http://www.20sim.com/>, 2008.